

# Autodeimination of Protein Arginine Deiminase 4 Alters Protein–Protein Interactions but Not Activity

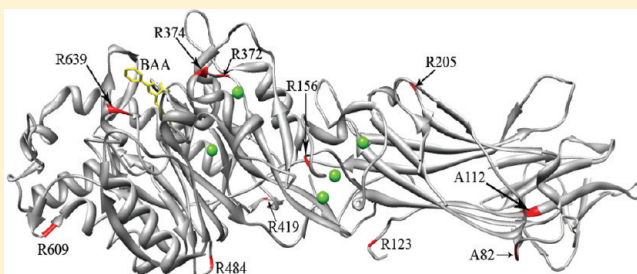
Jessica L. Slack,<sup>†,‡</sup> Larry E. Jones, Jr.,<sup>†</sup> Monica M. Bhatia,<sup>†</sup> and Paul R. Thompson<sup>\*,‡</sup>

<sup>†</sup>Department of Chemistry and Biochemistry, University of South Carolina, 631 Sumter Street, Columbia, South Carolina 29208, United States

<sup>‡</sup>Department of Chemistry, The Scripps Research Institute, 130 Scripps Way, Jupiter, Florida 33458, United States

 Supporting Information

**ABSTRACT:** The protein arginine deiminases (PAD), which catalyze the hydrolysis of peptidyl-arginine to form peptidyl-citrulline, play important roles in a variety of cell signaling pathways, including apoptosis, differentiation, and transcriptional regulation. In addition to these important cellular roles, PAD activity is dysregulated in multiple human diseases [e.g., rheumatoid arthritis (RA), cancer, and colitis], and significantly, PAD inhibition with Cl-amidine has been shown to reduce disease severity in the collagen-induced arthritis model of RA. Although these enzymes play important roles in human cell signaling and disease, the mechanisms that regulate PAD activity under both physiological and pathological conditions are poorly understood. One possible mechanism for regulating PAD activity is autodeimination, to which PAD4 has been shown by us and others to be subjected *in vitro* and *in vivo*. Herein, we demonstrate that PAD4 autodeimination does not alter the activity, substrate specificity, or calcium dependence of this isozyme. However, the results of these studies indicate a novel role for autodeimination in modulating the ability of PAD4 to interact with histone deacetylase 1 (HDAC1), citrullinated histone H3 (Cit H3), and protein arginine methyltransferase 1 (PRMT1).



Protein arginine deiminases (PADs) are a small group of protein-modifying enzymes that catalyze the hydrolysis of arginine residues to citrulline (Figure 1). This particular modification has gained much attention in recent years because of its apparent role in rheumatoid arthritis (RA) and, more recently, in cancer, multiple sclerosis, and colitis.<sup>1</sup> Although multiple PAD isozymes (e.g., PAD2 and -4) likely play a role in the aforementioned diseases, the fact that mutations in PAD4 confer an increased risk of developing RA in Asians, as well as the fact that PAD4 is overexpressed in the disease-associated tissues,<sup>2,3</sup> has focused most research, at the both the molecular and organismic level, on this isozyme. For example, inhibition of PAD activity with Cl-amidine, an inhibitor developed by our lab,<sup>4</sup> has been shown to reduce disease severity in the murine collagen-induced arthritis model of RA.<sup>5</sup> Cl-amidine treatment or siRNA knock-down of PAD4 has also been shown to induce either apoptosis or differentiation of a number of cancer-derived cell lines, including U2OS osteosarcoma cells (apoptosis), HL-60 leukemic cells (differentiation), and HT29 colon cancer cells (differentiation).<sup>6–9</sup> Additionally, PAD4 activity appears to play an important role in the innate immune response as the activity of this isozyme is required for the formation of neutrophil extracellular traps (NETs).<sup>10–13</sup> Finally, PAD4 is known to be recruited to the promoters of numerous genes where it deiminates histones H3 and H4, and this modification is associated with the decreased

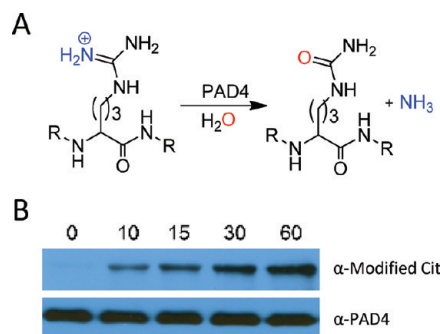


**Figure 1.** (A) PAD4-catalyzed reaction. (B) Autodeimination of PAD4. Recombinant PAD4 (0.2  $\mu$ M) was incubated in the presence of 10 mM calcium at 37 °C over a range of time points (0, 10, 15, 30, and 60 min). Citrullinated PAD4 was detected by Western blotting using the Anti-Modified Citrulline Detection Kit (top), and anti-PAD4 was used in the detection of PAD4 to demonstrate equal protein loading (bottom).

level of transcription of those genes via an unknown mechanism.<sup>6,7,14,15</sup>

**Received:** March 1, 2011

**Revised:** April 2, 2011

**Published:** April 05, 2011

Although our knowledge of the physiological roles of the PADs is improving, particularly with the development of inhibitors and chemical probes targeting these enzymes,<sup>4,16–21</sup> our understanding of the mechanisms that regulate PAD activity is less well developed, even though these enzymes are known to be calcium-dependent. This is particularly true when one considers the fact that high micromolar to millimolar concentrations of calcium are required to observe PAD activity *in vitro*. Such concentrations are far higher than the nanomolar to low micromolar concentrations of calcium found in a cell, where the PADs are clearly active.<sup>20</sup> Thus, it seems likely that additional factors regulate PAD activity *in vivo*. Potential higher-level regulatory mechanisms that could modulate PAD activity, as well as the amount of calcium required for *in vivo* activity, include both PAD-interacting proteins and PTMs. The latter possibility seems particularly plausible when one considers the fact that numerous cell signaling proteins are subject to multiple PTMs (e.g., phosphorylation, acetylation, and methylation) that regulate protein–protein interactions, enzymatic activity, and cellular localization. Given the putative role of PAD4 in human disease, understanding the mechanisms that regulate its deiminating activity, under both physiological and pathological conditions, is critical for a complete understanding of PAD4 function, as such knowledge will ultimately assist in the development of inhibitors targeting this enzyme.

Quite often, protein-modifying enzymes also modify themselves. As we and others<sup>22,23</sup> have shown, PAD4 is subject to autodeimination (Figure 1). As this modification could potentially regulate PAD activity, substrate specificity, calcium dependence, protein–protein interactions, and protein stability, we sought to understand the regulatory effects of PAD4 autodeimination at the molecular level. Herein, we report the identification of seven sites of autodeimination that occur both *in vitro* and *in vivo*. Site-directed mutagenesis was then used to probe the roles of these residues in regulating PAD4 activity, substrate specificity, calcium dependence, and protein–protein interactions. In contrast to a recent report,<sup>22</sup> the results of these studies indicate that autodeimination has minimal effects on the activity, substrate specificity, and calcium dependence of PAD4. However, we show for the first time that autodeimination alters the ability of PAD4 to bind to HDAC1, citrullinated histone H3 (Cit H3), and protein arginine methyltransferase 1 (PRMT1). In addition, we also investigated the effects of the RA-associated PAD4 haplotype, which consists of four exonic single-nucleotide polymorphisms that result in three amino acid substitutions: S55G, A82V, and A112G (the fourth polymorphism is silent). The results of these studies indicate that these substitutions also do not affect the activity, substrate specificity, or calcium dependence of PAD4. On the other hand, the SNPs appear to increase the affinity of PAD4 for Cit H3, H3, and HDAC1.

## MATERIALS AND METHODS

**Chemicals.** Dithiothreitol (DTT), iodoacetic acid, protease inhibitor cocktail (catalog no. P8465), and benzoyl L-arginine ethyl ester (BAEE) were acquired from Sigma-Aldrich (St. Louis, MO). Wild-type recombinant human PAD4 and wild-type recombinant human PRMT1 were purified using previously described methods.<sup>24,25</sup> Histones H3 and H4 were purified as previously described.<sup>26</sup> The synthesis and characterization of biotin-conjugated F-amidine (BFA), F-amidine-YNE, and TEV-biotin-azide have previously been described.<sup>20</sup>

**Construction of PAD4 Mutants and Purification of Recombinant Proteins.** The Quik Change Mutagenesis Kit (Stratagene) was used to introduce point mutations into the PAD4 gene. The sequences of the primers, which were obtained from IDT DNA Technologies, are listed in Table S1 of the Supporting Information. The entire open reading frame of each mutant gene was sequenced to ensure that the appropriate mutation was obtained without incorporation of undesired mutations. Expression and purification of the recombinant PAD4 mutants were conducted as previously described.<sup>24,27</sup>

**Purification of HDAC1 Fragment 1–90.** A recombinant *Escherichia coli* expression system encoding residues 1–90 of human HDAC1 (HDAC1 1–90) was a kind gift from F. Fuks. Briefly, the HDAC1 1–90 expression construct, which encodes the first 90 residues of human HDAC1 fused in frame to an N-terminal GST tag, was transformed into *E. coli* Rosetta cells (EMB Biosciences). A single colony was used to prepare starter cultures, which were used to inoculate 1 L of TB medium containing ampicillin (50  $\mu$ g/mL) and chloramphenicol (20  $\mu$ g/mL) in a 4 L baffled flask. Cells were incubated at 37 °C with shaking (250 rpm) until an OD<sub>600</sub> of 0.8 was reached. The culture was cooled to 16 °C, and IPTG (final concentration of 0.3 mM) was added to induce protein expression. After overnight incubation, the cells were harvested by centrifugation (5000 rpm for 10 min). The cell pellet was resuspended in 30 mL of lysis buffer [20 mM Tris-HCl (pH 8.0), 1 mM EDTA, 1 mM DTT, 400 mM NaCl, 20% glycerol, and protease inhibitor cocktail] and incubated for 30 min at 4 °C with gentle stirring. The cell suspension was then diluted with an additional 70 mL of lysis buffer and lysed by sonication (12 cycles with a 15 s burst, duty cycle 10, 100% output with 60 s intervals). Cellular debris was removed by centrifugation (14000 rpm for 30 min), and the supernatant was applied to a glutathione-Sepharose fast flow affinity column (GE Healthcare). The column was washed with 50 mL of low-salt buffer [20 mM Tris-HCl (pH 8.0), 1 mM EDTA, 1 mM DTT, 250 mM NaCl, and 10% glycerol], followed by 50 mL of high-salt buffer [20 mM Tris-HCl (pH 8.0), 1 mM EDTA, 1 mM DTT, 500 mM NaCl, and 10% glycerol]. GST-bound HDAC1 1–90 was eluted from the column with 25 mL of glutathione buffer [50 mM Tris-HCl (pH 8.0), 1 mM DTT, and 10 mM reduced glutathione]. Protein was dialyzed against 20 mM Tris-HCl (pH 7.6), 1 mM EDTA, and 2 mM DTT to remove any remaining glutathione. Dialyzed protein was applied to a S200 size exclusion column (GE Healthcare), and fractions were collected and analyzed via sodium dodecyl sulfate–polyacrylamide gel electrophoresis (SDS–PAGE). GST-bound HDAC1 1–90 was pooled and dialyzed against long-term storage buffer [20 mM Tris-HCl (pH 8.0), 2 mM DTT, 500 mM NaCl, and 10% glycerol], aliquoted, and stored at –80 °C.

**Kinetic Characterization of Mutant Enzymes.** All enzymatic assays were conducted as previously described.<sup>24</sup> Briefly, assays were performed in reaction buffer containing 100 mM Tris-HCl (pH 7.6), 50 mM NaCl, 2 mM DTT, and 10 mM CaCl<sub>2</sub> (final volume of 60  $\mu$ L). The reaction buffer containing the appropriate substrate (e.g., H4, H3, or BAEE) was preincubated for 10 min at 37 °C, followed by the addition of recombinant enzyme (final concentration of 0.2  $\mu$ M) to initiate the reaction. Citrulline production was quantified as previously described.<sup>24,28</sup> Experiments were performed at least in duplicate, and the values generally agreed to within 20%. The kinetic values (e.g.,  $k_{\text{cat}}$  and  $K_{\text{m}}$ ) were obtained by fitting the initial velocity data to the

Michaelis–Menten equation (eq 1)

$$v = V_{\max}[S]/(K_m + [S]) \quad (1)$$

using Graft version 5.0.11.<sup>29</sup>

**Calcium Dependence.** The calcium dependence of PAD4 mutants was characterized using methods that have previously been established for wild-type PAD4.<sup>24</sup> Briefly, reaction buffer, containing 100 mM Tris-HCl (pH 7.6), 50 mM NaCl, 2 mM DTT, 10 mM BAEE, and varying concentrations of CaCl<sub>2</sub> (0–10 mM), was preincubated for 10 min at 37 °C, followed by the addition of recombinant enzyme (final concentration of 0.2 μM) to initiate the reaction. After 15 min, the reactions were quenched and citrulline production was quantified as previously described.<sup>24</sup> The data obtained were fit to eq 2

$$v/V_{\max} = [Ca^{2+}]^n/(K_{0.5} + [Ca^{2+}]^n) \quad (2)$$

using Graft version 5.0.11,<sup>29</sup> where  $v$  is the initial rate,  $V_{\max}$  is the maximal rate, and  $K_{0.5}$  is the concentration of calcium that yields half-maximal activity.

**Autodeimination of PAD4.** Recombinant proteins were incubated in reaction buffer in the absence (no autodeimination) or presence (autodeimination) of 10 mM CaCl<sub>2</sub> at 37 °C and analyzed over a range of time points (from 0 to 60 min). Following this incubation, samples were boiled in SDS–PAGE loading buffer and subjected to electrophoresis on a 10% SDS–PAGE gel for 60 min at 200 V. Proteins were then electrotransferred onto a polyvinylidene difluoride (PVDF) membrane for 70 min at 80 V. Detection of autodeiminated PAD4 was accomplished using the Anti-Modified Citrulline Detection Kit (Upstate, Temecula, CA).

**Partial Proteolysis Experiments.** The partial proteolysis of wild-type PAD4 and PAD4 mutants was conducted as previously described.<sup>24</sup> Briefly, wild-type PAD4 and PAD4 mutants (0.2 μM) were incubated in the absence or presence of subtilisin (3.3 μg/mL) in reaction buffer on ice over a range of time points (0–60 min). The proteolysis reaction was quenched by the addition of phenylmethanesulfonyl fluoride (final concentration of 5 mM). Proteolytic fragments were separated via SDS–PAGE and visualized with Coomassie brilliant blue staining.

**Co-Immunoprecipitations.** Wild-type PAD4 and PAD4 mutants (5 μg) were labeled with 1 μM BFA for 30 min at 37 °C in reaction buffer. Labeled protein (5 μg) was added to MCF-7 whole cell extracts (500 μg of total protein) and applied to streptavidin–agarose beads (100 μL) and allowed to incubate overnight at 4 °C with end-over-end rocking. The beads were washed three times with PBS and then three times with NET-2 buffer [150 mM NaCl, 0.05% NP-40, and 50 mM Tris-HCl (pH 7.4)]. Beads were boiled in SDS buffer [2% SDS, 62.5 mM Tris-HCl (pH 6.8), and 10% glycerol], and then the eluted proteins were separated on a 12% SDS–PAGE gel and subsequently transferred to a nitrocellulose membrane. Membranes were probed with a mouse monoclonal anti-p53 antibody (Abcam, ab1101), a rabbit polyclonal anti-H3 antibody (Abcam, ab1791), anti-PRMT1 (Abcam, ab7027), anti-HDAC1 (Abcam, ab19845), and an anti-citrullinated H3 antibody (Abcam, ab77164).

**Stimulation of MCF-7 Cells.** MCF-7 cells were grown and maintained to 90% confluence in DMEM containing 10% FBS at 37 °C in 5% CO<sub>2</sub>, at which point the medium was exchanged with DMEM phenol red free containing 10% charcoal-stripped FBS. After incubation for 48 h at 37 °C in 5% CO<sub>2</sub>, estrogen

(0.1 μM) was added to stimulate the cells. After a 2 h incubation with estrogen, cells were rinsed in PBS and lysed in modified RIPA buffer [25 mM Tris-HCl (pH 7.6), 150 mM NaCl, 1% NP-40, and 1% sodium deoxycholate] containing a complete protease inhibitor tablet (Roche).

**Identification of Autodeimination Sites in Vitro.** Purified recombinant PAD4 (100 μg) was deiminated at 37 °C for 2 h in a standard reaction buffer containing 100 mM Tris-HCl (pH 7.6), 50 mM NaCl, and 2 mM DTT in the presence or absence of 10 mM CaCl<sub>2</sub>. For reactions performed in <sup>18</sup>O-labeled water, the PAD4 protein was lyophilized overnight, reconstituted in <sup>18</sup>O-labeled water, and incubated in reaction buffer under similar conditions. Autodeiminated sites were assessed from a tryptic digest of the autodeiminated samples followed by mass spectrometry analysis on an Ultraflex MALDI-TOF instrument (Bruker Daltonics). Briefly, autodeiminated samples were concentrated to 25 μL using micro spin columns (10000 molecular weight cutoff, Millipore) and mixed with 50 μL of denaturing buffer [6 M urea, 0.1 M MOPS, and 1 mM EDTA (pH 7.2)]. Protein was reduced and derivatized with 5 μM DTT (37 °C for 2 h) and 25 μM iodoacetamide (room temperature for 1 h), respectively. All reactions were performed on column, and the sample was mixed well by thorough pipetting before each step. To reduce the urea concentration, the buffer was washed off by centrifugation (5000g) and the column was then rinsed twice with 100 μL of water. Sequence-grade trypsin (Promega), which was reconstituted in 100 mM NH<sub>4</sub>HCO<sub>3</sub> (pH 8.0), was then added at a final enzyme:protein ratio of 1:20. Digestion was conducted overnight at 37 °C, and peptides were collected in the flow through in a fresh collection tube by centrifugation at 5000g for 20 min. Peptides were concentrated in a speedvac to a final volume of ~30 μL, desalted using a C<sup>18</sup> ZipTip (Millipore), and eluted in 2.5 μL of α-cyanohydroxycinnamic acid for analysis.

**Identification of Autodeimination Sites in Vivo.** HL-60 cells were differentiated along the granulocyte lineage with 1 μM all-*trans*-retinoic acid for 48 h. HL-60 granulocytes were incubated with F-amidine-YNE (final concentration of 100 μM) in the presence of a calcium ionophore, A23817 (4 μM), for 1 h at 37 °C in 5% CO<sub>2</sub>. Subsequently, the cells were harvested and lysed in modified RIPA buffer [25 mM Tris HCl (pH 7.6), 150 mM NaCl, 1% NP-40, and 1% sodium deoxycholate] containing a complete protease inhibitor tablet (Roche) on ice, for 10 min. The samples were denatured at 95 °C for 10 min prior to the addition of the TEV-biotin-azide (10 μM) reporter tag. The “click” reaction was then initiated by the addition of TCEP (2.5 mM), ligand {tris[(1-benzyl-1*H*-1,2,3-triazol-4-yl)methyl]-amine} (final concentration of 0.119 mM), and CuSO<sub>4</sub> (final concentration of 5 mM), as previously described.<sup>20,30</sup> After 1 h at room temperature, the protein samples were collected by centrifugation (5000 rpm and 4 °C), and the protein pellet was washed with cold methanol (2 × 100 μL). The protein pellet was resuspended in a 0.2% SDS/PBS mixture, added to 100 μL of streptavidin–agarose beads in PBS, and incubated overnight at 4 °C with end-over-end rocking. The beads were washed via addition of 500 μL of a 0.2% SDS/PBS mixture for 10 min and collected by centrifugation (1400g for 3 min). The supernatant was removed, and the beads were washed with PBS (3 × 5 mL). To elute the bound proteins, streptavidin–agarose beads were incubated in buffer A (2% SDS, 15 mM biotin, 100 mM thiourea, and 3 M urea in PBS) for 1 h at 42 °C followed by 30 min at 95 °C. The supernatant was then removed, and the beads were washed with water three times. The supernatant and wash



**Table 1. Steady-State Kinetic Parameters of Autodeiminated PAD4<sup>a</sup>**

	autodeimination for 1 h			autodeimination for 2 h		
	$k_{\text{cat}}$ (s <sup>-1</sup> )	$K_{\text{m}}$ (mM)	$k_{\text{cat}}/K_{\text{m}}$ (s <sup>-1</sup> M <sup>-1</sup> )	$k_{\text{cat}}$ (s <sup>-1</sup> )	$K_{\text{m}}$ (mM)	$k_{\text{cat}}/K_{\text{m}}$ (s <sup>-1</sup> M <sup>-1</sup> )
H4						
WT PAD4	2.1 ± 0.6	0.21 ± 0.10	10000	2.1 ± 0.6	0.21 ± 0.10	10000
adPAD4	0.6 ± 0.1	0.10 ± 0.04	6400	ND	ND	3000
conPAD4	1.0 ± 0.4	0.23 ± 0.13	4300	ND	ND	3000
H3						
WT PAD4	ND	ND	3700	ND	ND	3700
adPAD4	ND	ND	3500	ND	ND	3100
conPAD4	ND	ND	790	ND	ND	780
BAEE						
WT PAD4	2.8 ± 0.6	0.58 ± 0.12	4800	2.8 ± 0.6	0.58 ± 0.12	4800
adPAD4	2.7 ± 0.1	0.91 ± 0.14	3000	1.0 ± 0.1	3.8 ± 0.6	250
conPAD4	2.6 ± 0.1	0.69 ± 0.07	3800	0.9 ± 0.1	2.5 ± 0.89	340

<sup>a</sup> Recombinant wild-type (WT) PAD4 (0.2 μM) was incubated in the absence (conPAD4) or presence (adPAD4) of 10 mM calcium for 1 or 2 h at 37 °C. The kinetic parameters were then determined by incubating enzyme with H4, H3, and BAEE over a range of concentrations at 37 °C for 6 min. Abbreviations: WT PAD4, nonincubated protein; adPAD4, autodeiminated PAD4; conPAD4, non-autodeiminated incubated control; ND, not determined.

factions were combined and concentrated to approximately 20 μL. The entire sample was loaded onto a 12% SDS–PAGE gel, and proteins were visualized by Coomassie blue staining. A protein band corresponding to the approximate molecular weight of PAD4 was excised from the gel and subjected to an in-gel tryptic digestion. In-gel digestion was performed as previously described.<sup>31</sup> Peptides were concentrated in a speedvac to a final volume of ~30 μL, desalted using a C<sup>18</sup> ZipTip (Millipore), and eluted in 2.5 μL of α-cyanohydroxycinnamic acid for analysis on an Ultraflex MALDI-TOF instrument (Bruker Daltonics).

## RESULTS AND DISCUSSION

**Autodeimination of PAD4 in Vitro.** Many enzymes that generate PTMs also modify themselves as a mode of regulating their enzymatic activity. Given this fact, we were interested in determining whether PAD4 autodeiminated. For these studies, wild-type recombinant PAD4 was incubated in the absence ( $t = 0$  min) or presence of calcium ( $t = 10, 15, 30$ , and 60 min) for various lengths of time, and the presence of citrullinated residues was detected by Western blotting using an anti-modified citrulline antibody. The results of these studies indicated that PAD4 is autodeiminated in a time-dependent manner with near-maximal deimination occurring at the 60 min time point (Figure 1B). These results are consistent with those obtained by Andrade et al.<sup>22</sup>

**Effects of Autodeimination on PAD4 Activity.** To investigate the effects of autodeimination on PAD4 activity, we determined the steady-state kinetic parameters for a variety of small molecule and protein substrates (i.e., histones H3 and H4, as well as BAEE), using both recombinant PAD4 and autodeiminated PAD4 (adPAD4); adPAD4 was generated by incubating the enzyme in the presence of 10 mM calcium for 1 h. To control for the effects of incubation time on PAD4 activity, we also incubated PAD4 in the absence of calcium for 1 h to generate control PAD4 (conPAD4). As shown in Table 1, the kinetic parameters obtained for BAEE, H3, and H4 with adPAD4 are generally comparable to those obtained with PAD4 and

conPAD4; the effects on  $k_{\text{cat}}/K_{\text{m}}$  are ≤2.3-fold. The one exception to this trend is the result obtained with H3. Here, incubation in the absence of calcium led to a 4.7-fold reduction in  $k_{\text{cat}}/K_{\text{m}}$ . However, when the enzyme was incubated for 1 h in the presence of calcium, little to no change in  $k_{\text{cat}}/K_{\text{m}}$ , relative to that of PAD4, was observed. The reasons for this small, but nonetheless significant, loss of activity for H3 are unclear, but overall, the results are inconsistent with the notion that autodeimination negatively impacts PAD4 activity.

Given that Andrade et al. previously suggested that the autodeimination of PAD4 inhibits its deiminating activity,<sup>22</sup> we were understandably concerned with our results. The major differences between our two studies are (i) the incubation time (2 h in their study vs 1 h in ours) and (ii) the choice of substrate (Andrade et al. used HL-60 cell extracts as PAD4 substrates and detected changes in protein citrullination using the anti-modified citrulline antibody). To determine whether the incubation time could explain the discrepancy, we determined the kinetic parameters for adPAD4 and conPAD4 after a 2 h incubation in the presence and absence of calcium. The results of these studies (Table 1) indicate that there was little to no difference in the kinetic parameters obtained for adPAD4 and conPAD4 that were incubated for 2 h. The one exception is again the case of H3, for which the  $k_{\text{cat}}/K_{\text{m}}$  for H3 with conPAD4 is ~4-fold lower than that obtained with adPAD4. Again, while the reason for this discrepancy is not known, the effect is relatively weak. It is interesting to note, however, that significant activity is lost after the enzyme is incubated for 2 h as compared to WT PAD4. For example, a pronounced decrease in  $k_{\text{cat}}/K_{\text{m}}$  was observed with both H4 (~3.3-fold) and BAEE (~14–19-fold) after the 2 h incubation (compare the data for adPAD4 and conPAD4 to those for the nonincubated control) (Table 1). The fact that both adPAD4 and conPAD4 are less active after the 2 h incubation suggests that the loss of activity is nonspecific in nature. This seems likely given the fact that the loss of activity is less pronounced at the 1 h time point. Taken together, these results indicate that autodeimination of PAD4 has little to no effect on the steady-state kinetic parameters of PAD4, at least in vitro.

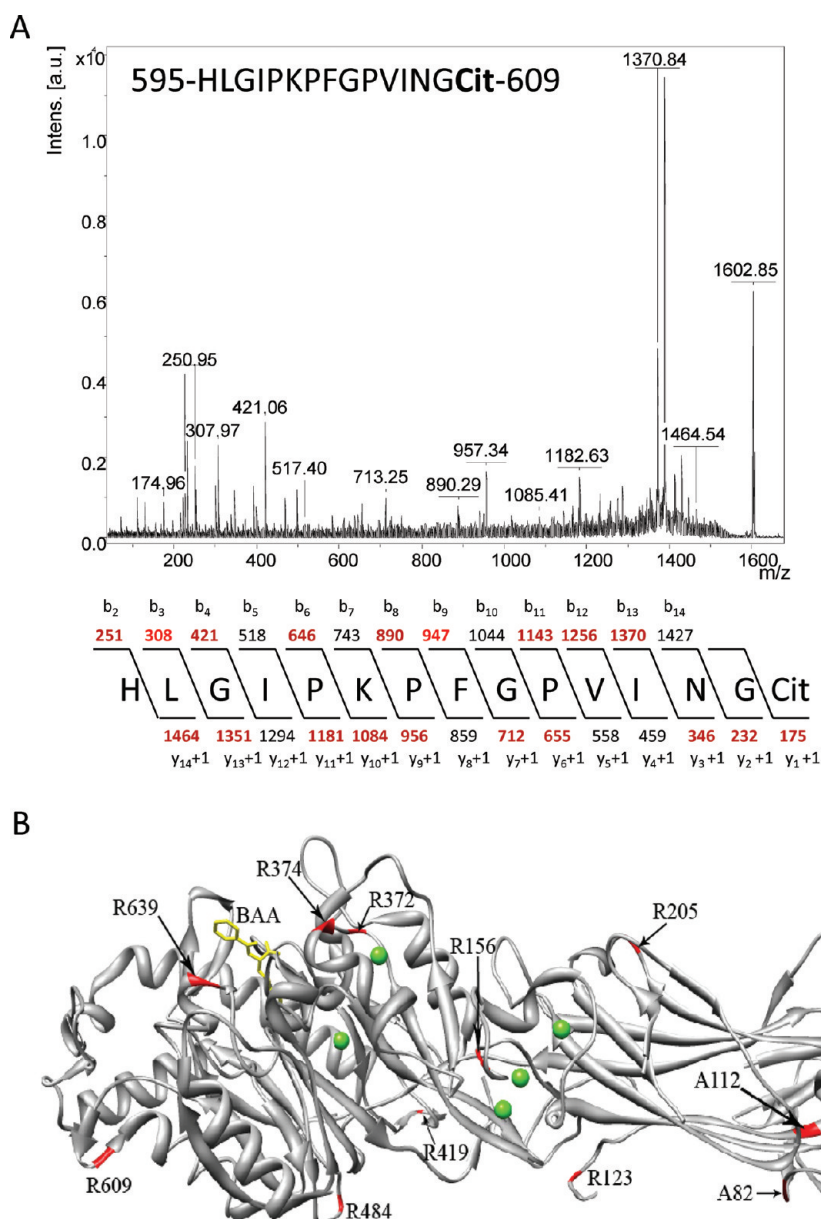


**Figure 2.** (A) Representative mass spectrometry data for autodeimination sites found in PAD4. (B) Location of PAD4 AD sites and SNPs. The crystal structure was generated using UCSF Chimera<sup>37</sup> and Protein Data Bank entry 1WDA.<sup>32</sup> The locations of the deiminated arginines and the SNPs are colored red on the ribbon structure. Bound calcium ions (spheres) are colored green, and BAA (benzoyl-L-arginine amide) is colored yellow.

Given that Andrade et al. had used whole cell extracts as the source of proteins for their activity measurements, we hypothesized that a protein present in those extracts, or some other unknown component, could potentially be acting to inhibit PAD4 activity. To examine this possibility, we prepared whole cell extracts from unstimulated and estrogen-stimulated MCF-7 cells (MCF-7 cells are from a breast adenocarcinoma-derived cell line that is known to express PAD4) and examined the effects of these extracts on the kinetic parameters of adPAD4 and conPAD4. The results of these studies (Figure S1 and Table S2 of the Supporting Information) indicate that neither extract altered the activity of PAD4 as the  $k_{\text{cat}}/K_m$  values obtained with adPAD4 and conPAD4 are virtually identical. Thus, there appears to be no endogenous factor in MCF-7 cell extracts that can inhibit PAD4 activity. Although it is unclear why we see such dramatically

different results, it is worth noting that Andrade et al. used very small amounts of  $\beta$ -mercaptoethanol in their incubation buffers, and the observed loss of activity may be due to oxidation of the active site Cys, as we and others have previously shown that enzyme activity is highly dependent on the presence of a reducing agent.<sup>24,28</sup>

**Effect of Autodeimination on the Calcium Dependence of PAD4.** Given that PAD4 requires millimolar amounts of calcium for activity *in vitro*<sup>24</sup> but only nanomolar to low millimolar levels of calcium are found *in vivo*, we were curious to see whether autodeimination could alter the calcium dependence of this enzyme. For these studies, adPAD4 was generated by incubating the enzyme in reaction buffer with 10 mM calcium for either 1 or 2 h. The excess calcium was then removed by dialysis, and then PAD4 activity was measured as a function of the increasing level

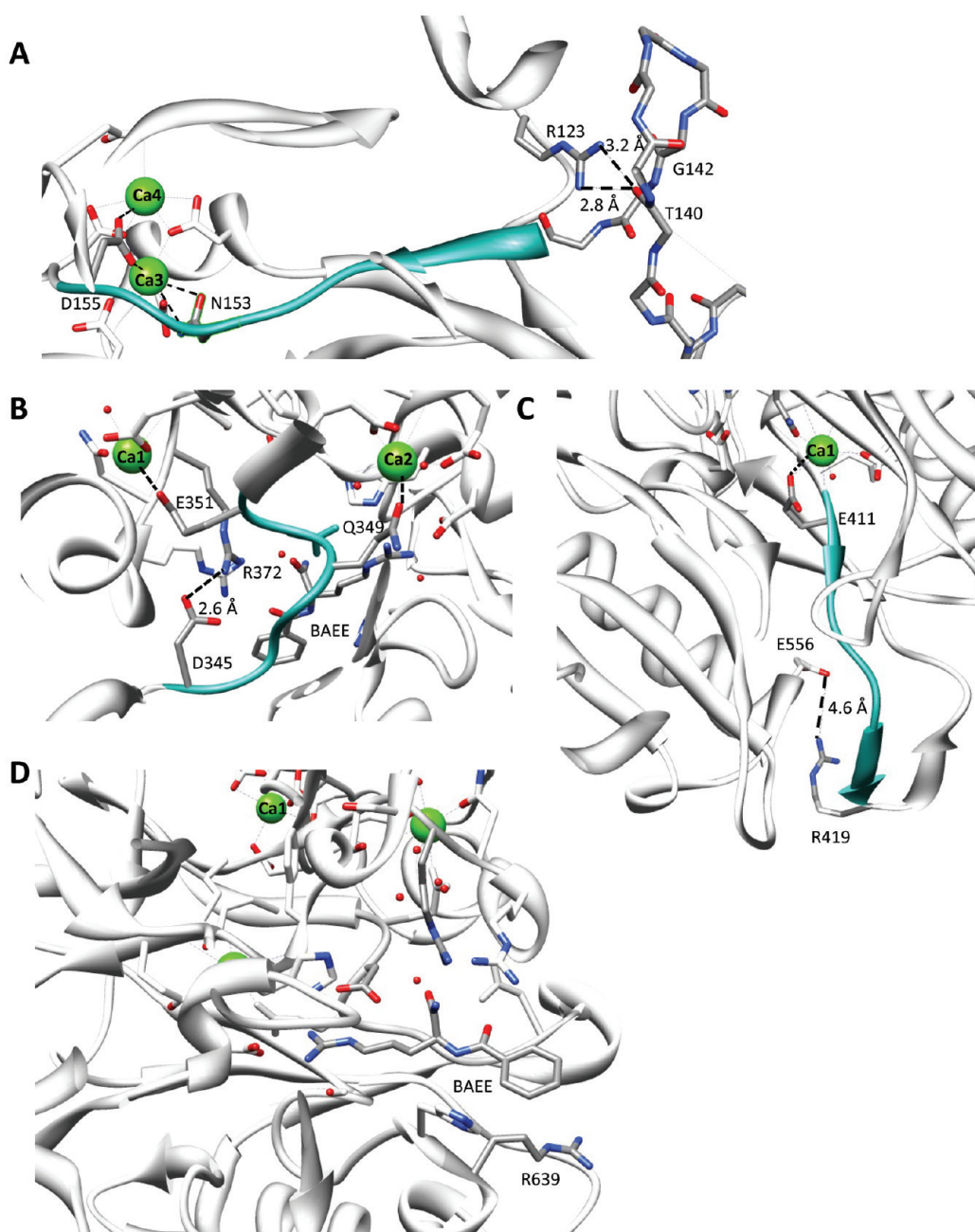


**Figure 3.** Structural basis for the effects of autodeimination on the activity and calcium dependence of PAD4. (A) R123. This image shows a close-up of the region surrounding R123 and highlights its proximity to calciums 3 and 4 and its interaction with the backbone carbonyl of T140. (B) R372. This image highlights the interactions between R372 and D345 and how disruption of this interaction might alter the position of D350, a key catalytic residue. (C) R419. Proximity of R419 to E556. This panel shows a close-up of the R419–E556 interaction. Disruption of this interaction would be expected to disrupt the stability of the  $\beta$ -strands linked to E411, a ligand for calcium 1. (D) R639. This panel highlights the position of R639 in the structure of the PAD4·calcium·BAA complex. Note that calcium ions are spheres and BAA is shown in elemental colors. These panels were generated using UCSF Chimera<sup>37</sup> and Protein Data Bank entry 1WDA.

of calcium. Because the activity versus calcium concentration plots are sigmoidal, the data were fit to the Hill equation to provide values for the Hill coefficient ( $n$ ) and  $K_{0.5}$  for calcium activation (Figure S2 of the Supporting Information). The results of these studies indicated that when PAD4 was autodeiminated for 1 h no significant effect was present on either the  $K_{0.5}$  or the Hill coefficient ( $K_{0.5} = 407 \pm 106 \mu\text{M}$ ;  $n = 2.3 \pm 0.37$ ) compared to those of the nonincubated control ( $K_{0.5} = 500 \pm 91 \mu\text{M}$ ;

$n = 1.5 \pm 0.37$ ). Similar results were obtained when PAD4 was autodeiminated for 2 h ( $K_{0.5} = 1200 \pm 170$ ;  $n = 2.0 \pm 0.37$ ). Although the  $K_{0.5}$  is increased by 2.4-fold with this treatment, the effect is relatively small and inconsistent with the hypothesis that autodeimination could decrease the concentration of calcium required for PAD4 activity. Taken together, the data suggest that autodeimination has little to no effect on the calcium dependence of PAD4.



**Table 2. Steady-State Kinetic Parameters of PAD4 Mutants<sup>a</sup>**

	H4			BAEE		
	$k_{\text{cat}}$ (s <sup>-1</sup> )	$K_{\text{m}}$ (mM)	$k_{\text{cat}}/K_{\text{m}}$ (s <sup>-1</sup> M <sup>-1</sup> )	$k_{\text{cat}}$ (s <sup>-1</sup> )	$K_{\text{m}}$ (mM)	$k_{\text{cat}}/K_{\text{m}}$ (s <sup>-1</sup> M <sup>-1</sup> )
wild type	2.1 ± 0.64	0.21 ± 0.10	10000	2.8 ± 0.58	0.58 ± 0.12	4800
R123K	1.7 ± 0.52	0.24 ± 0.11	7100	3.7 ± 0.06	0.86 ± 0.05	4300
R123Q	0.90 ± 0.15	0.10 ± 0.03	9000	2.3 ± 0.12	1.4 ± 0.24	1600
R156K	1.4 ± 0.27	0.18 ± 0.06	7800	0.76 ± 0.03	0.50 ± 0.08	1500
R156Q	0.79 ± 0.17	0.11 ± 0.05	7200	3.6 ± 0.27	1.6 ± 0.37	2200
R205K	ND <sup>b</sup>	ND <sup>b</sup>	3700	3.8 ± 0.21	1.5 ± 0.27	2500
R205Q	ND <sup>b</sup>	ND <sup>b</sup>	2100	1.2 ± 0.04	0.48 ± 0.07	2500
R372K	ND <sup>b</sup>	ND <sup>b</sup>	≤3.1	ND <sup>b</sup>	ND <sup>b</sup>	≤0.6 × 10 <sup>-6</sup>
R372Q	ND <sup>b</sup>	ND <sup>b</sup>	≤12.0	ND <sup>b</sup>	ND <sup>b</sup>	≤1.0 × 10 <sup>-6</sup>
R374K	0.49 ± 0.08	0.088 ± 0.03	5600	3.0 ± 0.18	1.7 ± 0.31	1800
R374Q	0.77 ± 0.05	0.15 ± 0.02	5100	2.3 ± 0.16	1.2 ± 0.28	1900
R419K	1.3 ± 0.32	0.14 ± 0.06	9300	3.1 ± 0.23	0.72 ± 0.21	4300
R419Q	1.2 ± 0.32	0.22 ± 0.09	5500	0.55 ± 0.02	0.87 ± 0.14	630
R484K	1.6 ± 0.35	0.26 ± 0.08	6200	1.1 ± 0.05	0.45 ± 0.10	2400
R484Q	1.6 ± 0.40	0.30 ± 0.10	5300	1.2 ± 0.09	0.45 ± 0.16	2700
R609K	ND <sup>b</sup>	ND <sup>b</sup>	4900	2.6 ± 0.26	1.5 ± 0.49	1700
R609Q	1.5 ± 0.1	0.18 ± 0.02	8300	1.9 ± 0.07	0.89 ± 0.11	2100
R639K	1.3 ± 0.19	0.15 ± 0.04	8700	1.9 ± 0.14	0.69 ± 0.20	2800
R639Q	0.78 ± 0.10	0.094 ± 0.02	8300	1.6 ± 0.09	1.2 ± 0.23	1300

<sup>a</sup> Kinetic parameters determined by incubating enzyme (0.2 μM) with substrates H4 and BAEE over a range of concentrations at 37 °C for 6 min. <sup>b</sup> Not Determined.

**Identification of the Sites of Autodeimination.** MS analyses were used to identify the sites of PAD4 autodeimination, both in vitro and in vivo. To identify the in vitro sites of deimination, recombinant PAD4 was either reconstituted in <sup>18</sup>O-labeled water and autodeiminated for 2 h or autodeiminated directly for 2 h. Subsequently, adPAD4 was subjected to in-solution tryptic digestion and MS and MS/MS analyses. Note that we performed these experiments in <sup>18</sup>O-labeled water to enhance our ability to identify the sites of autodeimination because deimination in normal water results in an only 0.98 Da mass increase, whereas in <sup>18</sup>O-labeled water, an ~3 Da increase is observed. The results of these studies identified six in vitro sites of autodeimination, i.e., R123, R156, R205, R419, R484, and R639 (Table S3 of the Supporting Information). Note that sequence coverage was 64%. To identify the sites of autodeimination that occur in vivo, we isolated endogenous PAD4 from HL-60 granulocytes utilizing a recently described PAD4-targeted ABPP, i.e., F-amidine-YNE.<sup>20</sup> For these studies, F-amidine-YNE (final concentration of 100 μM), in the presence of a calcium ionophore (i.e., A23817, final concentration of 4 μM), was added to HL-60 granulocytes for 1 h. Subsequently, the cells were harvested, lysed, and then denatured by being boiled at 95 °C for 10 min. The TEV-biotin-azide reporter tag was then added in the presence of TCEP, ligand, and copper sulfate to afford the coupling of the reporter tag to F-amidine-YNE via the copper-catalyzed azide-alkyne [3+2] cycloaddition reaction. Biotinylated proteins were then isolated on streptavidin-agarose beads, eluted, and separated via SDS-PAGE. A band corresponding to the size of PAD4 was excised from the gel and subjected to in-gel tryptic digestion. The results of these studies identified two in vivo sites (i.e., R123 and R609) of autodeimination (see Figure 2A for representative MS data). As depicted in Figure 2B, the majority of the autodeiminated arginine residues clustered in the C-terminal

catalytic domain (i.e., R419, R484, R609, and R639), while the three remaining arginines are located in the N-terminus of the protein (i.e., R123, R156, and R205). Note that all of these residues are not directly accessible to the active site; thus, the deimination of these residues must occur in trans. Also note that while Andrade et al. identified 10 sites of autodeimination (i.e., R205, R212, R218, R372, R374, R383, R394, R495, R536, and R544), only one of these sites, i.e., R205, is shared between these two analyses. The reason for this discrepancy is unknown but may be related to the different methods of detection (LC-MS and MS/MS vs MALDI-TOF/TOF) or the fact that we do not observe an effect of autodeimination on PAD4 activity.

**Site-Directed Mutagenesis.** Site-directed mutagenesis was next used to investigate the contribution of these autodeiminated residues to the in vitro activity and calcium dependence of PAD4. To mimic the effects of arginine deimination, R123, R156, R205, R419, R484, R609, and R639, as well as R372 and R374 (previously described sites of autodeimination<sup>22</sup>), were mutated to glutamine, and the steady-state kinetic parameters were determined for BAEE and histone H4. Although the side chain of glutamine is approximately two methylene units shorter than the side chain of citrulline, we considered that the carboxamide moiety present on glutamine would provide a reasonable mimic of the ureido group in citrulline as it possesses similar hydrogen bond acceptors and donors. These residues were also mutated to lysine to serve as nondeiminatable controls. As shown in Table 3, only minor effects on the kinetic parameters are observed when R123, R156, R205, R484, R609, R639, and R374 are mutated to either a glutamine or a lysine. These results are consistent with our results demonstrating that autodeimination has only minor effects on PAD4 activity. The two exceptions are the data obtained for the R372 mutants and the R419Q mutant when

**Table 3. Calcium Dependence of PAD4 Mutants<sup>a</sup>**

	N	$K_{0.5}$ ( $\mu$ M)
wild type	1.5 $\pm$ 0.19	500 $\pm$ 91
R123K	2.2 $\pm$ 0.25	106 $\pm$ 29
R123Q	4.5 $\pm$ 0.55	310 $\pm$ 66
R156K	1.4 $\pm$ 0.36	410 $\pm$ 150
R156Q	2.2 $\pm$ 0.24	550 $\pm$ 83
R205K	3.8 $\pm$ 0.61	105 $\pm$ 46
R205Q	2.9 $\pm$ 0.65	109 $\pm$ 61
R372K	ND <sup>b</sup>	ND <sup>b</sup>
R372Q	ND <sup>b</sup>	ND <sup>b</sup>
R374K	2.8 $\pm$ 0.51	230 $\pm$ 83
R374Q	1.8 $\pm$ 0.14	420 $\pm$ 51
R419K	2.4 $\pm$ 0.26	66 $\pm$ 23
R419Q	2.1 $\pm$ 0.56	300 $\pm$ 140
R484K	2.6 $\pm$ 0.22	320 $\pm$ 47
R484Q	2.6 $\pm$ 0.37	380 $\pm$ 89
R609K	1.9 $\pm$ 0.39	480 $\pm$ 140
R609Q	1.7 $\pm$ 0.25	530 $\pm$ 106
R639K	2.4 $\pm$ 0.77	85 $\pm$ 75
R639Q	3.2 $\pm$ 0.81	100 $\pm$ 67

<sup>a</sup> Values were obtained by incubating protein (0.2  $\mu$ M) and BAEE (10 mM) over a range of calcium concentrations (0–10 mM) at 37 °C for 10 min. <sup>b</sup> Not determined.

BAEE is used as the substrate (see below). The effect of these arginine substitutions on the calcium dependence of PAD4 was also analyzed. For the R156, R374, R484, and R609 mutants, only very minor effects on the Hill coefficient and  $K_{0.5}$  for calcium were observed. The exceptions are the data obtained for R123, R205, R419, and R639. The effects of mutating these residues, as well as R372, on the calcium dependence and activity of PAD4 are described below. Note that partial proteolysis experiments were performed on all of the PAD4 mutants described. The fact that the behavior of these mutants was identical to that of the wild-type enzyme in these assays indicates that the observed changes in activity are not due to gross structural perturbations. Also note that while we generally define minor effects as being  $\leq 2$ -fold, we recognize that such small effects in vitro could potentially have profound effects in vivo. Nevertheless, to limit speculation, we have generally focused our discussion on only  $\geq 2$ -fold changes.

**R123.** R123 is present on the tip of a loop in subdomain 1 (Figure 3A) and likely stabilizes a second loop encompassing residues 138–146 via hydrogen bond interactions with the backbone carbonyls of T140 ( $r = 2.8$  Å) and G142 ( $r = 3.2$  Å). As deimination of this residue would be expected to disrupt these interactions, one might expect that this would lead to the destabilization of this loop. Given that this loop directly connects to the region of the enzyme that binds to calciums 1, 2, and 3, one might further expect that its deimination would alter the calcium dependence of the enzyme. Consistent with this notion is the fact that the  $K_{0.5}$  for calcium obtained for the R123Q mutant ( $K_{0.5} = 310 \pm 66$   $\mu$ M) is significantly higher than that obtained with the R123K mutant ( $K_{0.5} = 106 \pm 29$   $\mu$ M), which mimics a nondeiminatable arginine. While the  $K_{0.5}$  of the R123K mutant is significantly lower than that observed for the wild-type enzyme ( $\sim 5$ -fold), it remains higher than physiologically relevant. Thus, deimination of this residue cannot fully explain the in vitro requirement for such high levels of calcium.

**R205.** Mutation of R205 to either a lysine or a glutamine decreases the  $k_{\text{cat}}/K_m$  for histone H4 and BAEE by 4.8- and 2.7-fold, respectively. Additionally, these mutations reduce the  $K_{0.5}$  for calcium by  $\sim 5$ -fold. Although the molecular basis for these effects is not known, it may be due to effects on dimerization as R205 is present on a short loop connecting  $\beta$ -strand 12 in subdomain 2 to helix  $\alpha 4$  and appears to form hydrogen bonds with the backbone carbonyl and amide groups of S437, the second subunit in the PAD4 dimer. As such, the inability to form the correct hydrogen bonding patterns, which would be expected with both mutants, would be expected to at least partially destabilize the PAD4 dimer.

**R372.** Although we did not observe autodeimination of R372, we were interested in determining the importance of this residue because Andrade et al. had suggested that this residue is deiminated and that its mutation to a lysine abolished PAD4 activity. Consistent with previous results,<sup>22,32</sup> the conversion of R372 to either a lysine or glutamine resulted in a  $>830$ -fold decrease in  $k_{\text{cat}}/K_m$  when either BAEE or histone H4 was tested as the substrate (Table 2). Given the magnitude of these effects, which essentially decreased the activity to baseline, it was not possible to examine the effect of these mutations on the calcium dependence of PAD4. On the basis of the structure of PAD4, there are at least two possible reasons for the loss of activity. First, R372 forms a water-mediated hydrogen bond to the backbone carbonyl C-terminal to the site of deimination (Figure 3B), and loss of this interaction would be expected to increase the  $K_m$  for the substrate. Second, when bound to calcium, the side chain guanidinium of R372 forms an electrostatic interaction with D345 that likely helps position D350, an essential active site residue,<sup>27</sup> so that it can bind and orient the substrate guanidinium for nucleophilic attack by the active site cysteine, i.e., C645. This interaction likely occurs in a calcium-dependent manner because N373, which is one residue C-terminal to R372, acts a ligand for calcium 2. Given the magnitude of the effect of mutating this residue on PAD4 activity, which is on the order of mutating D350, the latter explanation seems most likely.

**R419.** With respect to the activity of the R419Q mutant, the  $k_{\text{cat}}/K_m$  obtained for BAEE is decreased 7.6-fold relative to that of the wild-type enzyme, whereas the R419K mutant maintains near wild-type activity (Table 3). As the decrease in  $k_{\text{cat}}/K_m$  is driven mostly by an  $\sim 5$ -fold decrease in  $k_{\text{cat}}$ , these results suggest that the loss of activity may be due to an inability to properly adopt the active conformation of the enzyme. However, the fact that a  $<2$ -fold effect on  $k_{\text{cat}}/K_m$  is observed when histone H4 is used as a substrate suggests that long-range interactions between the enzyme and the substrate can compensate for the loss of the positively charged side chain of R419.

With respect to the calcium dependence of the R419 mutants, the  $K_{0.5}$  of the R419K mutant ( $66 \pm 23$   $\mu$ M) is decreased by 7.6-fold relative to that of the wild-type enzyme ( $500 \pm 91$   $\mu$ M) (Table 3), whereas the values obtained for the glutamine mutant are similar to those obtained for wild-type PAD4 ( $300 \pm 140$   $\mu$ M). As the glutamine mutant mimics a constitutively deiminated form of the enzyme, these data are consistent with the notion that the deimination of R419 could increase the  $K_{0.5}$  for calcium. To provide a molecular basis for this effect, we examined the structure of PAD4 bound to calcium and found that this residue, which is present on the  $\beta$ -turn that connects  $\beta$ -strand 26 and  $\beta$ -strand 27, points toward the C-terminus of helix  $\alpha 12$  and likely stabilizes the structure of the helix via electrostatic interactions with the helix dipole. Additional stabilization likely comes



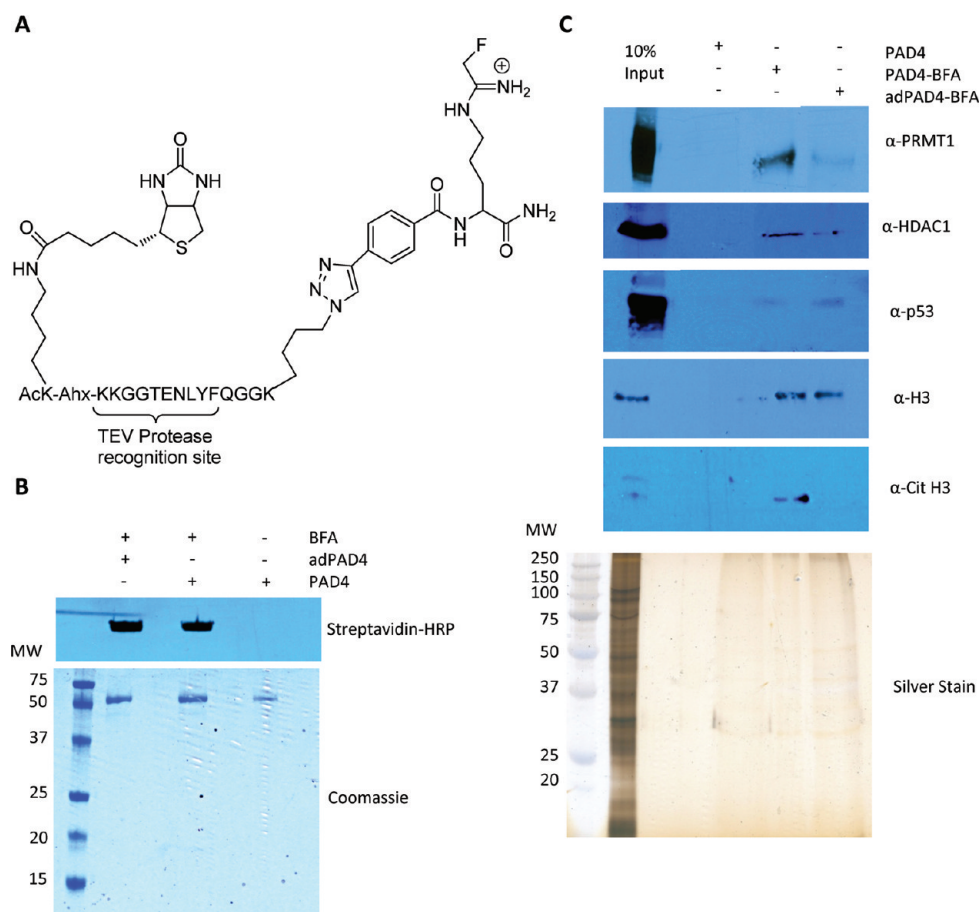


**Figure 4.** (A) Structure of BFA. (B) Labeling of conPAD4 and adPAD4 with BFA. (C) Enrichment of PAD4 binding proteins using conPAD4-BFA and adPAD4-BFA. conPAD4-BFA and adPAD4-BFA were incubated with MCF-7 WCE to isolate known PAD4 binding proteins, including H3, Cit H3, HDAC1, and PRMT1. The proteins were enriched on streptavidin–agarose beads and analyzed by Western blotting.

via an electrostatic interaction with E556, which is present at the C-terminus of this helix (Figure 3C). These two interactions also likely stabilize the structure of  $\beta$ -strand 26. Given that R419 is only eight residues C-terminal to E411 (E411 is present on  $\beta$ -strand 25, binds to calcium 1, and appears to be essential for activity), the deimination of this residue could destabilize this region of PAD4 and potentially increase the amount of calcium required to trigger the conformational change that converts PAD4 from an inactive to active conformation. If true, such a mechanism would explain the results obtained with the R419K mutant, a nondeiminatable PAD4 mutant, and that lysine can act as a functional mimic of the arginine residue at this position.

**R639.** Mutation of R639 to either a lysine or a glutamine also decreased the  $K_{0.5}$  for calcium by  $\sim 5$ -fold. This residue, which lines the top of the substrate binding cleft on helix  $\alpha 16$ , points out into solution and is far from the sites of calcium binding (Figure 3D). Thus, it is unclear how the mutation of this residue leads to a weakened requirement for calcium. It is, however, worth noting that the fact that this residue lines the substrate binding cleft suggests that the deimination of this residue could impact PAD4 substrate recognition, although that does not appear to be the case with either BAEE or histone H4.

**Autodeimination of PAD4 Weakens Protein–Protein Interactions.** Given our results showing that autodeimination has only minor effects on the catalytic activity and calcium dependence of PAD4, we hypothesized that this PTM may indirectly

affect PAD4 activity by altering its ability to interact with its binding partners. This seems reasonable when one considers that the deimination of arginine residues results in a net loss of positive charge, and such a change can have profound effects on local electrostatic interactions and hydrogen bonding with proximal residues or with potential binding proteins. To examine this possibility, we investigated the ability of adPAD4 to co-immunoprecipitate with known PAD4 binding proteins from stimulated MCF-7 WCE. Wild-type PAD4 was autodeiminated at 37 °C for 1 h and labeled with BFA, a recently described PAD4-targeted activity-based protein profiling (ABPP) reagent (Figure 4A).<sup>20</sup> Wild-type nondeiminated PAD4 was labeled with BFA in an identical fashion (Figure 4B). The labeled protein was then used to “fish” out known binding proteins from the extracts. The PAD4 binding proteins evaluated were histone H3, Cit H3, p53, HDAC1, and PRMT1. Note that while PRMT1 has not previously been shown to be a PAD4 binding protein, co-immunoprecipitation experiments were used to confirm this finding (Figure S3 of the Supporting Information). The results of these experiments indicated that the binding affinities of adPAD4 for p53 and H3 were similar to those of nondeiminated PAD4 (Figure 5). In contrast, the affinities of adPAD4 for HDAC1, PRMT1, and Cit H3 were reduced by 3.7-, 4.5-, and  $>10$ -fold, respectively (Figure 5). These results suggest that the autodeimination of PAD4 in vivo could affect its functional activity by regulating its ability to interact with binding partners.

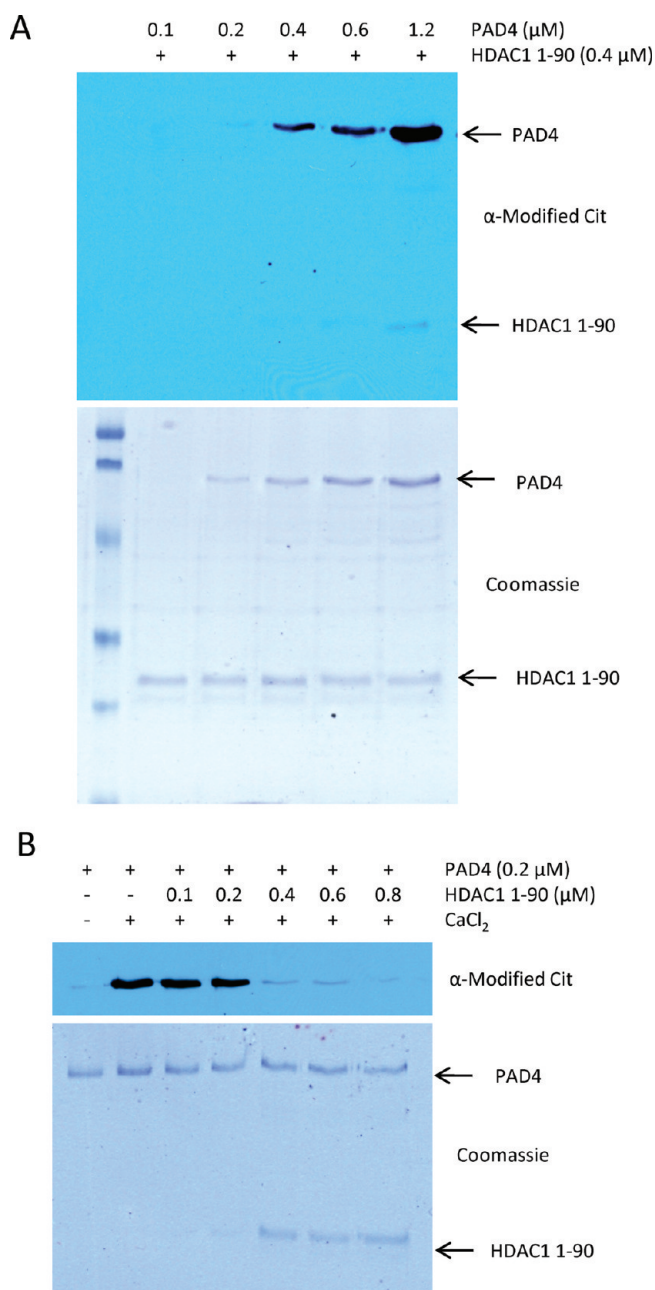


**Figure 5.** (A) HDAC1 is a poor PAD4 substrate. HDAC1 (0.4  $\mu\text{M}$ ) was incubated with increasing amounts of PAD4 (0.1–1.2  $\mu\text{M}$ ) for 30 min at 37  $^{\circ}\text{C}$ . Modification of HDAC1 by PAD4 was monitored by Western blotting using an anti-modified citrulline antibody. (B) HDAC1 protects PAD4 from autodeimination. PAD4 was incubated for 60 min at 37  $^{\circ}\text{C}$  with increasing amounts of HDAC1 1–90 (0.1–0.8  $\mu\text{M}$ ). Autodeimination of PAD4 was monitored by Western blotting using the anti-modified citrulline antibody.

Given the fact that the autodeimination of PAD4 weakens its ability to bind to a subset of the aforementioned proteins, we reasoned that one or more of these proteins could protect the enzyme from autodeimination. To test this hypothesis, we determined whether HDAC1 1–90 could inhibit PAD4 autodeimination. Note that we focused on this enzyme because it is a weak PAD4 substrate (see Figure 5A), whereas both H3 and PRMT1 (unpublished results) are PAD4 substrates. Thus, if

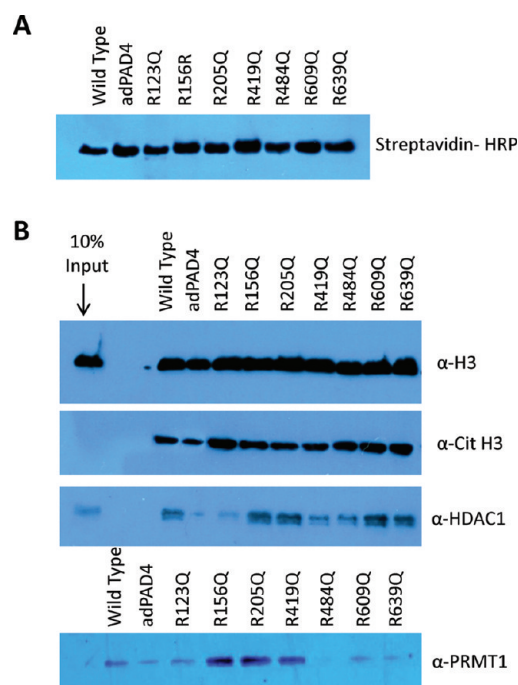


**Figure 6.** Enrichment of PAD4 binding proteins using adPAD4 substitution mutants. (A) BFA-labeled WT PAD4 and adPAD4 mutants were subjected to Western blotting using streptavidin-bound HRP to demonstrate equal protein loading. (B) adPAD4 substitution mutants prelabeled with BFA were incubated with MCF-7 WCE overnight at 4  $^{\circ}\text{C}$  to enrich PAD4 binding proteins, i.e., H3, Cit H3, HDAC1, and PRMT1. Enrichment of these proteins on streptavidin–agarose beads was monitored by Western blot analysis.

autodeimination was prevented in the presence of HDAC1 1–90, it would most likely be due to the binding of PAD4 and not the addition of a competing substrate. For these studies, increasing amounts of HDAC1 1–90 were incubated in the presence of PAD4 and the autodeimination reaction was allowed to proceed for 1 h. The results of these studies indicated that HDAC1 1–90 does indeed prevent PAD4 autodeimination (Figure 5B). The fact that PAD4 autodeimination is almost completely blocked by the addition of a 2-fold molar excess of HDAC1 1–90 suggests that HDAC1 1–90 binds a PAD4 monomer as a dimer.

**Co-Immunoprecipitation of PAD4 Mutants with Binding Partners.** To identify the key residues responsible for mediating the interaction between PAD4 and Cit H3, HDAC1, and PRMT1, we investigated whether the glutamine substitution mutants could co-immunoprecipitate these proteins. Note that we focused on using the glutamine mutants, as opposed to the lysine mutants, because deimination reduced the level of binding of these proteins to PAD4 and this substitution mimics a constitutively deiminated arginine residue. Also note that H3 was used as a control. For these studies, the R123Q, R156Q, R205Q, R419Q, R484Q, R609Q, and R639Q substitution mutants were labeled with BFA (Figure 6A) and incubated with MCF-7 WCE, and their ability to isolate the aforementioned proteins was evaluated by Western blotting. As expected, the affinity for H3 is unchanged by the substitution mutants for no effect was seen with adPAD4. Similar results were obtained for Cit H3, suggesting that additive, or even synergistic, interactions from multiple autodeiminated arginine residues lower the affinity

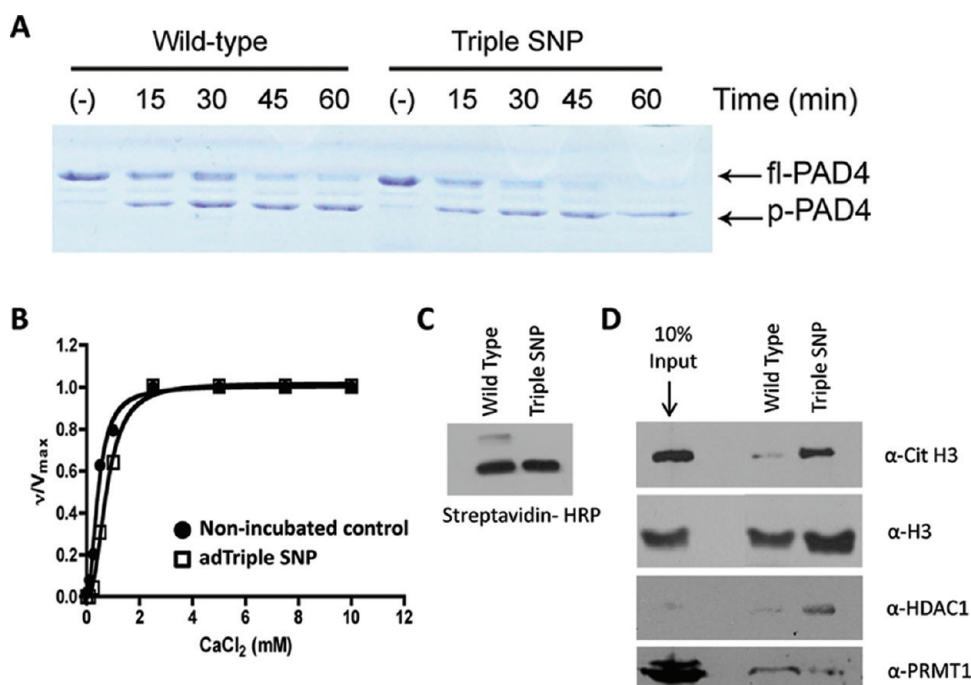


**Figure 7.** (A) Partial proteolysis of recombinant PAD4 and the triple SNP. Recombinant PAD4 and the triple SNP ( $2\ \mu\text{g}$ ) were incubated with subtilisin ( $3.3\ \mu\text{g/mL}$ ) on ice over a range of time points (0–60 min). Samples were boiled in SDS loading buffer, run on a 10% SDS–PAGE gel, and stained with Coomassie blue. (B) Calcium dependence of the autodeiminated triple SNP. The triple SNP ( $2\ \mu\text{M}$ ) was incubated in the presence of 10 mM calcium for 1 h ( $\square$ ) at  $37^\circ\text{C}$ , followed by dialysis to remove calcium and then a determination of the calcium dependence in comparison to that of the nonincubated positive control ( $\bullet$ ) at  $37^\circ\text{C}$  over a range of calcium concentrations (0–10 mM) using BAEE as the substrate. The graph shows a Hill plot of  $v/V_{max}$  vs calcium concentration. (C) Streptavidin-bound HRP Western blot demonstrating equal loading and equal labeling of wild-type PAD4 and the triple SNP with BFA. (D) The triple SNP and wild-type PAD4 prelabeled with BFA were incubated with MCF-7 WCE overnight at  $4^\circ\text{C}$  to enrich them with H3, Cit H3, HDAC1, and PRMT1. Enrichment of these proteins on streptavidin–agarose beads was observed by Western blot analysis.

of PAD4 for Cit H3 (Figure 6B). In contrast to these results, significant differences in the binding of these mutant enzymes to HDAC1 and PRMT1 were observed. For example, the affinities of HDAC1 for the R123Q, R419Q, and R484Q mutants are decreased by 3.3-, 1.4-, and 1.4-fold, respectively. For PRMT1, the effects are more dramatic, with the affinities of the R123Q, R484Q, R609Q, and R639Q mutants for PRMT being reduced by 2-, 10-, 3.3-, and 5-fold, respectively (Figure 6). These results indicate that these sites of deimination are likely critical for forming high-affinity interactions between PAD4 and these proteins. With respect to HDAC1, these results are at least partially consistent with the results of Fuks and colleagues, who showed that HDAC1 interacts mainly with the C-terminus of PAD4 (residues 400–631), where R419 and R484 are located.<sup>33</sup>

**Characterization of PAD4 SNPs.** Four exonic single-nucleotide polymorphisms (SNPs) are present in the PAD4 gene, and these SNPs have been shown to confer an increased risk of developing RA, at least in Asian populations.<sup>34,35</sup> Three of these SNPs result in amino acid substitutions (i.e., S55G, A82V, and A112G), and the fourth is silent. Note that all three residues are present in N-terminal subdomain 1, and because no electron density was observed for S55, its position in the crystal structure is estimated (Figure 2). Initially, we sought to examine the effects of these SNPs on protein stability and activity by generating PAD4 constructs containing the individual SNP site and a construct containing all three substitutions (triple SNP). To examine the stability of these mutants, we performed partial proteolysis experiments. For these studies, the S55G, A82V, and A112G mutants, as well as the triple SNP, were incubated with

subtilisin over a range of time points. For the single mutants, incubation with subtilisin produced a pattern of degradation that was similar to that of the wild-type protein. In contrast, the triple SNP mutant appeared to be slightly less stable than the wild type, as it was more susceptible to being proteolyzed into smaller fragments (Figure 7A).

To investigate the effects of these SNPs on PAD4 activity, the steady-state kinetic parameters were determined for the S55G, A82V, and A112G single mutants, as well as the triple SNP, using both BAEE and histone H4 as the substrates. The results of these studies indicated that mutation of these residues has only minor effects on the activity of PAD4; the  $k_{cat}/K_m$  values are either not affected (as in the case of the S55G mutant) or decreased by only 1.7–2.5- and 2.3–3.2-fold for histone H4 and BAEE, respectively (Table 4). The effects of these mutations on the calcium dependence are similarly weak (Table 5).

**Autodeimination of the Triple SNP.** It has previously been shown that autodeimination of the triple SNP and wild-type PAD4 occurs with similar kinetics and that the relative activities of these two enzymes are similar;<sup>22,36</sup> however, detailed kinetic analyses have not been performed. Therefore, the steady-state kinetic parameters were determined for the autodeiminated form of the triple SNP using BAEE and histones H3 and H4 as the substrates. The results of these experiments revealed that autodeimination of the triple SNP leads to only modest effects on the kinetic parameters (Table 6). The loss of activity compared to that of the nonincubated control is likely due to nonspecific time-dependent inactivation of the enzyme, as described above. The calcium dependence of the autodeiminated triple SNP was also



**Table 4. Steady-State Kinetic Parameters of PAD4 SNPs<sup>a</sup>**

	H4			BAEE		
	$k_{\text{cat}}$ (s <sup>-1</sup> )	$K_m$ (mM)	$k_{\text{cat}}/K_m$ (s <sup>-1</sup> M <sup>-1</sup> )	$k_{\text{cat}}$ (s <sup>-1</sup> )	$K_m$ (mM)	$k_{\text{cat}}/K_m$ (s <sup>-1</sup> M <sup>-1</sup> )
wild type	2.1 ± 0.64	0.21 ± 0.10	10000	2.8 ± 0.58	0.58 ± 0.12	4800
S55G	1.1 ± 0.18	0.20 ± 0.05	5500	2.8 ± 0.21	0.44 ± 0.15	6400
A82V	1.4 ± 0.47	0.35 ± 0.16	4000	2.7 ± 0.17	1.3 ± 0.27	2100
A112G	1.0 ± 0.24	0.17 ± 0.07	5900	1.5 ± 0.12	0.80 ± 0.23	1900
triple SNP	1.3 ± 0.54	0.24 ± 0.15	5400	2.9 ± 0.40	2.0 ± 0.74	1500

<sup>a</sup> Kinetic parameters determined by incubating enzyme (0.2 μM) with substrates H4 and BAEE over a range of concentrations at 37 °C for 6 min. The triple SNP contains all three mutations (S55G, A82V, and A112G).

**Table 5. Calcium Dependence of PAD4 SNPs<sup>a</sup>**

	$N$	$K_{0.5}$ (μM)
wild type	1.5 ± 0.19	500 ± 91
S55G	2.3 ± 0.43	240 ± 90
A82V	3.2 ± 0.48	204 ± 66
A112G	1.8 ± 0.42	550 ± 180
triple SNP	2.0 ± 0.56	180 ± 108

<sup>a</sup> Values were obtained by incubating protein (0.2 μM) and BAEE (10 mM) over a range of calcium concentrations (0–10 mM) at 37 °C for 10 min. The triple SNP contains all three substitutions (S55G, A82V, and A112G).

examined, and the results indicate that the  $K_{0.5}$  is increased by 2.9-fold ( $K_{0.5} = 520 \pm 67 \mu\text{M}$ ;  $n = 2.4 \pm 0.2$ ) (Figure 7B). In total, these data indicate that autodeimination does not have a significant effect on either the steady-state kinetic parameters or the calcium dependence of the triple SNP.

**Co-Immunoprecipitation of the Triple SNP and PAD4 Binding Proteins.** To investigate whether the triple SNP alters interactions with known PAD4 binding proteins, co-immunoprecipitation experiments were performed. For these studies, the triple SNP and wild-type PAD4 were labeled with BFA (Figure 7C) and incubated with MCF-7 WCE, and their ability to isolate H3, Cit H3, HDAC1, and PRMT1 was evaluated by Western blot analysis. Interestingly, the triple SNP had a higher affinity for H3, Cit H3, and HDAC1. In contrast, there was little to no change in the affinity of the Triple SNP for PRMT1 (Figure 7D). Although speculative, these results could partially explain some of the observed differences between the RA haplotype and wild-type PAD4. For example, if the triple SNP has a higher affinity for H3, it could potentially lead to higher rates of histone deimination *in cellulo*, which would be expected to promote NET formation. Given that PAD4 and HDAC1 are known to work together to repress gene transcription,<sup>33</sup> the higher affinity of the triple SNP for HDAC1 could also lead to the enhanced repression of genes required to resolve or constrain the inflammatory response.

## CONCLUSIONS

Enzymes in eukaryotic cells are regulated by a number of multilayered and interconnected mechanisms. From transcription of the new mRNA, to alternative RNA splicing, to translation, to further modification by select PTMs, these mechanisms work to continuously fine-tune a protein's activity in a variety of cellular environments. Of the various regulatory mechanisms, PTMs serve a particular niche by being highly dynamic, being

**Table 6. Steady-State Kinetic Parameters of the Autodeiminated Triple SNP<sup>a</sup>**

	$k_{\text{cat}}$ (s <sup>-1</sup> )	$K_m$ (mM)	$k_{\text{cat}}/K_m$ (s <sup>-1</sup> M <sup>-1</sup> )
<b>H4</b>			
triple SNP control	1.3 ± 0.54	0.24 ± 0.15	5400
ad-triple SNP	ND	ND	4600
con-triple SNP	ND	ND	1700
<b>H3</b>			
triple SNP control	ND	ND	3700
ad-triple SNP	ND	ND	3000
con-triple SNP	ND	ND	2200
<b>BAEE</b>			
triple SNP control	2.9 ± 0.40	2.0 ± 0.74	1500
ad-triple SNP	0.90 ± 0.03	0.89 ± 0.12	1000
con-triple SNP	0.74 ± 0.09	1.2 ± 0.48	620

<sup>a</sup> Recombinant protein (0.2 μM) was incubated in the absence or presence of 10 mM calcium for 1 h at 37 °C, followed by the assay. Kinetic parameters were determined by incubating enzyme with substrates H4, H3, and BAEE over a range of concentrations at 37 °C for 6 min. Abbreviations: triple SNP control, nonincubated protein; ad-triple SNP, autodeiminated form; con-triple SNP, non-autodeiminated form; ND, not determined.

largely reversible, and modifying functionally important residues and can have profound effects on physiological processes. Given that the enzymes involved in regulating gene transcription possess multiple PTMs that regulate their activity, PAD4, which is a transcriptional corepressor, is likely to also possess PTMs that regulate its activity. As such, understanding the mechanisms that regulate PAD4 activity under physiological and pathological conditions is a high priority because the activity of this enzyme is aberrantly increased in several human diseases (e.g., RA, cancer, and colitis).

As we (this work) and others have reported,<sup>22</sup> PAD4 autodeiminates *in vitro* and *in vivo*. Given the potential role of this PTM in regulating PAD4 activity, we investigated the effect of autodeimination on the activity and calcium dependence of PAD4. In contrast to a previous report,<sup>22</sup> we found that autodeimination does not have pronounced effects on the activity of the enzyme. Note that this observation was independently verified by three different researchers. Although it is difficult to speculate about the specific reasons for these starkly different results, we did observe a nonspecific time-dependent partial loss of activity when PAD4 was incubated at 37 °C for 2 h. However, in our hands, this effect is independent of autodeimination. It is also possible that the different results are due to differences in the

methodology used to assess PAD4 activity. For example, we directly determined the steady-state kinetic parameters of PAD4 and adPAD4 using a highly defined and well-established enzyme assay system with highly purified substrates. In contrast, Andrade et al. used HL-60 cell lysates as the source of substrate proteins and quantified changes in activity by Western blotting using an anti-modified citrulline antibody. Thus, it is possible that a protein, ion, or small molecule present in the HL-60 cell extracts could promote the autodeimination of a different pattern of arginine residues (including, for example, R372) that favors enzyme inactivation.

To further confirm our findings, we identified six sites in PAD4 that were autodeiminated (i.e., R123, R156, R205, R419, R484, and R639) and used site-directed mutagenesis to establish the roles of these residues in controlling the activity and calcium dependence of PAD4. Consistent with our finding that autodeimination of PAD4 does not affect the activity or calcium dependence of the enzyme, we did not observe any pronounced effects on either parameter when these residues were mutated to either a glutamine or lysine, each of which mimics constitutively deiminated or nondeiminated arginine residues, respectively. We also investigated whether the RA-associated PAD4 haplotype alters the activity of this isozyme. Consistent with recent reports,<sup>22,36</sup> only minor effects on the activity and calcium dependence of PAD4 were observed.

Given that autodeimination of PAD4 and the triple SNP does not strongly affect the activity and calcium dependence of PAD4, we hypothesized that these modifications might affect interactions between PAD4 and PAD4 binding proteins. Consistent with this possibility is our observation that the interaction between adPAD4 and PRMT1, citH3, and HDAC1 is significantly weakened. In contrast, the triple SNP shows enhanced binding to H3, Cit H3, and HDAC1. Although these interacting proteins do not significantly alter the activity or calcium dependence of PAD4 (not shown), it is likely that by modulating the ability of PAD4 to interact with these proteins, it is possible to alter downstream cell signaling pathways. For example, autodeimination of PAD4 may destabilize a corepressor complex consisting of PAD4 and HDAC1, thereby providing a mechanism for decreasing the corepressor activity of this complex. With respect to the triple SNP, the enhanced binding affinity for HDAC1 could oppose the effects of autodeimination, thereby leading to the stabilization of this complex, which would be expected to enhance gene repression. As it pertains to RA, this effect may lead to the enhanced repression of genes required to resolve or constrain the inflammatory response. Future studies to define how autodeimination affects these interactions in vivo will undoubtedly improve our understanding of the role of PAD4 in both physiological and pathological processes.

## ■ ASSOCIATED CONTENT

**S Supporting Information.** Tables S1–S4 and Figures S1–S3. This material is available free of charge via the Internet at <http://pubs.acs.org>.

## ■ AUTHOR INFORMATION

### Corresponding Author

\*Department of Chemistry, The Scripps Research Institute, 130 Scripps Way, Jupiter, FL 33458. Telephone: (561) 228-2471. Fax: (561) 228-3050. E-mail: [pthompson@scripps.edu](mailto:pthompson@scripps.edu).

### Author Contributions

J.L.S. and L.E.J. contributed equally to this work.

### Funding Sources

This work was supported by National Institutes of Health Grant GM079357 to P.R.T.

## ■ ABBREVIATIONS

PAD, protein arginine deiminase; Cit, citrulline; RA, rheumatoid arthritis; BAEE, benzoyl-L-arginine ethyl ester; DTT, dithiothreitol; TCEP, tris(2-carboxyethyl)phosphine; EDTA, ethylenediaminetetraacetic acid; PRMT, protein arginine methyltransferase; HDAC1, histone deacetylase 1; Cit H3, citrullinated histone H3; BFA, biotin-conjugated F-aminidine; PTMs, post-translational modifications; SNP, single-nucleotide polymorphism.

## ■ REFERENCES

- (1) Jones, J. E., Causey, C. P., Knuckley, B., Slack-Noyes, J. L., and Thompson, P. R. (2009) Protein arginine deiminase 4 (PAD4): Current understanding and future therapeutic potential. *Curr. Opin. Drug Discovery Dev.* 12, 616–627.
- (2) Lee, Y. H., Rho, Y. H., Choi, S. J., Ji, J. D., and Song, G. G. (2007) PAD14 polymorphisms and rheumatoid arthritis susceptibility: A meta-analysis. *Rheumatol. Int.* 27, 827–833.
- (3) Gandjbakhch, F., Fajardy, I., Ferre, B., Dubucquoi, S., Flipo, R. M., Roger, N., and Solau-Gervais, E. (2009) A Functional Haplotype of PAD14 Gene in Rheumatoid Arthritis: Positive Correlation in a French Population. *J. Rheumatol.* 36, 881–886.
- (4) Luo, Y., Arita, K., Bhatia, M., Knuckley, B., Lee, Y. H., Stallcup, M. R., Sato, M., and Thompson, P. R. (2006) Inhibitors and inactivators of protein arginine deiminase 4: Functional and structural characterization. *Biochemistry* 45, 11727–11736.
- (5) Willis, V., Gizinski, A., Knuckley, B., Causey, C. P., Luo, Y., Banda, N., Thompson, P. R., and Holers, V. M. (2011) Efficacy of Cl-aminidine in the collagen induced model of rheumatoid arthritis. *J. Immunol.* 186, 4396–4404.
- (6) Li, P., Yao, H., Zhang, Z., Li, M., Luo, Y., Thompson, P. R., Gilmour, D. S., and Wang, Y. (2008) Regulation of p53 target gene expression by peptidylarginine deiminase 4. *Mol. Cell. Biol.* 28, 4745–4758.
- (7) Yao, H., Li, P., Venters, B. J., Zheng, S., Thompson, P. R., Pugh, B. F., and Wang, Y. (2008) Histone Arg modifications and p53 regulate the expression of OKL38, a mediator of apoptosis. *J. Biol. Chem.* 283, 20060–20068.
- (8) Liu, G. Y., Liao, Y. F., Chang, W. H., Liu, C. C., Hsieh, M. C., Hsu, P. C., Tsay, G. J., and Hung, H. C. (2006) Overexpression of peptidylarginine deiminase IV features in apoptosis of haematopoietic cells. *Apoptosis* 11, 183–196.
- (9) Slack, J. L., Causey, C. P., and Thompson, P. R. (2011) Protein arginine deiminase 4: A target for an epigenetic cancer therapy. *Cell. Mol. Life Sci.* 68, 709–720.
- (10) Neel, J., Khan, S. N., and Radic, M. (2008) Histone deimination as a response to inflammatory stimuli in neutrophils. *J. Immunol.* 180, 1895–1902.
- (11) Wang, Y., Li, M., Stadler, S., Correll, S., Li, P., Wang, D., Hayama, R., Leonelli, L., Han, H., Grigoryev, S. A., Allis, C. D., and Coonrod, S. A. (2009) Histone hypercitrullination mediates chromatin decondensation and neutrophil extracellular trap formation. *J. Cell Biol.* 184, 205–213.
- (12) Li, P., Li, M., Lindberg, M. R., Kennett, M. J., Xiong, N., and Wang, Y. (2010) PAD4 is essential for antibacterial innate immunity mediated by neutrophil extracellular traps. *J. Exp. Med.* 207, 1853–1862.
- (13) Marcos, V., Zhou, Z., Yildirim, A. O., Bohla, A., Hector, A., Vitkov, L., Wiedenbauer, E. M., Krautgartner, W. D., Stoiber, W., Belohradsky, B. H., Rieber, N., Kormann, M., Koller, B., Roscher, A.,

Roos, D., Griesse, M., Eickelberg, O., Doring, G., Mall, M. A., and Hartl, D. (2010) CXCR2 mediates NADPH oxidase-independent neutrophil extracellular trap formation in cystic fibrosis airway inflammation. *Nat. Med.* 16, 1018–1023.

(14) Cuthbert, G. L., Daujat, S., Snowden, A. W., Erdjument-Bromage, H., Hagiwara, T., Yamada, M., Schneider, R., Gregory, P. D., Tempst, P., Bannister, A. J., and Kouzarides, T. (2004) Histone deimination antagonizes arginine methylation. *Cell* 118, 545–553.

(15) Wang, Y., Wysocka, J., Sayegh, J., Lee, Y. H., Perlin, J. R., Leonelli, L., Sonbuchner, L. S., McDonald, C. H., Cook, R. G., Dou, Y., Roeder, R. G., Clarke, S., Stallcup, M. R., Allis, C. D., and Coonrod, S. A. (2004) Human PAD4 Regulates Histone Arginine Methylation Levels via Demethylation. *Science* 306, 279–283.

(16) Knuckley, B., Jones, J. E., Bachovchin, D. A., Slack, J., Causey, C. P., Brown, S. J., Rosen, H., Cravatt, B. F., and Thompson, P. R. (2010) A fluopol-ABPP HTS assay to identify PAD inhibitors. *Chem. Commun.* 46, 7175–7177.

(17) Knuckley, B., Luo, Y., and Thompson, P. R. (2008) Profiling Protein Arginine Deiminase 4 (PAD4): A novel screen to identify PAD4 inhibitors. *Bioorg. Med. Chem.* 16, 739–745.

(18) Luo, Y., Knuckley, B., Bhatia, M., and Thompson, P. R. (2006) Activity Based Protein Profiling Reagents for Protein Arginine Deiminase 4 (PAD4): Synthesis and in vitro Evaluation of a Fluorescently-labeled Probe. *J. Am. Chem. Soc.* 128, 14468–14469.

(19) Luo, Y., Knuckley, B., Lee, Y. H., Stallcup, M. R., and Thompson, P. R. (2006) A Fluoro-Acetamidine Based Inactivator of Protein Arginine Deiminase 4 (PAD4): Design, Synthesis, and in vitro and in vivo Evaluation. *J. Am. Chem. Soc.* 128, 1092–1093.

(20) Slack, J. L., Causey, C. P., Luo, Y., and Thompson, P. R. (2011) The Development and Use of Clickable Activity Based Protein Profiling Agents for Protein Arginine Deiminase 4. *ACS Chem Biol.*, in press.

(21) Knuckley, B., Causey, C. P., Jones, J. E., Bhatia, M., Dreyton, C. J., Osborne, T. C., Takahara, H., and Thompson, P. R. (2010) Substrate specificity and kinetic studies of PADs 1, 3, and 4 identify potent and selective inhibitors of protein arginine deiminase 3. *Biochemistry* 49, 4852–4863.

(22) Andrade, F., Darrah, E., Gucek, M., Cole, R. N., Rosen, A., and Zhu, X. (2010) Autocitrullination of human peptidyl arginine deiminase type 4 regulates protein citrullination during cell activation. *Arthritis Rheum.* 62, 1630–1640.

(23) Mechin, M. C., Coudane, F., Adoue, V., Arnaud, J., Duplan, H., Charveron, M., Schmitt, A. M., Takahara, H., Serre, G., and Simon, M. (2010) Deimination is regulated at multiple levels including auto-deimination of peptidylarginine deiminases. *Cell. Mol. Life Sci.* 67, 1491–1503.

(24) Kearney, P. L., Bhatia, M., Jones, N. G., Luo, Y., Glascock, M. C., Catchings, K. L., Yamada, M., and Thompson, P. R. (2005) Kinetic characterization of protein arginine deiminase 4: A transcriptional corepressor implicated in the onset and progression of rheumatoid arthritis. *Biochemistry* 44, 10570–10582.

(25) Obianyo, O., Osborne, T. C., and Thompson, P. R. (2008) Kinetic mechanism of protein arginine methyltransferase 1. *Biochemistry* 47, 10420–10427.

(26) Thompson, P. R., Kurooka, H., Nakatani, Y., and Cole, P. A. (2001) Transcriptional coactivator protein p300. Kinetic characterization of its histone acetyltransferase activity. *J. Biol. Chem.* 276, 33721–33729.

(27) Knuckley, B., Bhatia, M., and Thompson, P. R. (2007) Protein arginine deiminase 4: Evidence for a reverse protonation mechanism. *Biochemistry* 46, 6578–6587.

(28) Knipp, M., and Vasak, M. (2000) A colorimetric 96-well microtiter plate assay for the determination of enzymatically formed citrulline. *Anal. Biochem.* 286, 257–264.

(29) Leatherbarrow, R. J. (2004) *Grafit*, version 5.0, Erathicus Software, Staines, U.K.

(30) Weerapana, E., Speers, A. E., and Cravatt, B. F. (2007) Tandem orthogonal proteolysis-activity-based protein profiling (TOP-ABPP): A

general method for mapping sites of probe modification in proteomes. *Nat. Protoc.* 2, 1414–1425.

(31) Shevchenko, A., Tomas, H., Havlis, J., Olsen, J. V., and Mann, M. (2006) In-gel digestion for mass spectrometric characterization of proteins and proteomes. *Nat. Protoc.* 1, 2856–2860.

(32) Arita, K., Shimizu, T., Hashimoto, H., Hidaka, Y., Yamada, M., and Sato, M. (2006) Structural basis for histone N-terminal recognition by human peptidylarginine deiminase 4. *Proc. Natl. Acad. Sci. U.S.A.* 103, 5291–5296.

(33) Denis, H., Deplus, R., Putmans, P., Yamada, M., Metivier, R., and Fuks, F. (2009) Functional connection between deimination and deacetylation of histones. *Mol. Cell. Biol.* 29, 4982–4993.

(34) Suzuki, A., Yamada, R., Chang, X., Tokuhiro, S., Sawada, T., Suzuki, M., Nagasaki, M., Nakayama-Hamada, M., Kawada, R., Ono, M., Ohtsuki, M., Furukawa, H., Yoshino, S., Yukioka, M., Tohma, S., Matsubara, T., Wakitani, S., Teshima, R., Nishioka, Y., Sekine, A., Iida, A., Takahashi, A., Tsunoda, T., Nakamura, Y., and Yamamoto, K. (2003) Functional haplotypes of PADI4, encoding citrullinating enzyme peptidylarginine deiminase 4, are associated with rheumatoid arthritis. *Nat. Genet.* 34, 395–402.

(35) Kang, C. P., Lee, H. S., Ju, H., Cho, H., Kang, C., and Bae, S. C. (2006) A functional haplotype of the PADI4 gene associated with increased rheumatoid arthritis susceptibility in Koreans. *Arthritis Rheum.* 54, 90–96.

(36) Horikoshi, N., Tachiwana, H., Saito, K., Osakabe, A., Sato, M., Yamada, M., Akashi, S., Nishimura, Y., Kagawa, W., and Kurumizaka, H. (2011) Structural and biochemical analyses of the human PAD4 variant encoded by a functional haplotype gene. *Acta Crystallogr. D* 67, 112–118.

(37) Pettersen, E. F., Goddard, T. D., Huang, C. C., Couch, G. S., Greenblatt, D. M., Meng, E. C., and Ferrin, T. E. (2004) UCSF Chimera: A visualization system for exploratory research and analysis. *J. Comput. Chem.* 25, 1605–1612.